

## Scaling of voltage-current characteristics of thin-film Y-Ba-Cu-O at low magnetic fields

J. M. Roberts, Brandon Brown, B. A. Hermann,\* and J. Tate

Department of Physics, Oregon State University, Corvallis, Oregon 97331-6507

(Received 22 November 1993)

We have measured voltage-current characteristics for  $\text{YBa}_2\text{Cu}_3\text{O}_7$  thin films in magnetic fields from 5 T to ambient, including some in the millitesla range. In all cases, the resistivity-current density isotherms can be separated into two classes: those which exhibit upward curvature, and have constant resistivity at low currents, and those which exhibit downward curvature at all currents. These two classes of isotherms are separated by a field-dependent temperature  $T_g$ . For each field, the isotherms scale in a manner consistent with a three-dimensional vortex-liquid to vortex-glass phase transition. The region that can be scaled is several kelvin at 5 T and narrows with decreasing field. The low-current resistivity above  $T_g$  varies as  $|1 - T/T_g|^s$  with  $s \approx 7.4$  at all fields, but the critical scaling exponents  $z$  and  $\nu$  become field dependent below about 10 mT.

### I. INTRODUCTION

A series of recent experiments<sup>1-5</sup> has provided support for the conjecture<sup>6</sup> that the flux lines in high-temperature superconductors undergo a phase transition from a liquidlike to a glassy state at a temperature  $T_g$  below the superconducting transition temperature  $T_c$ .<sup>7</sup> This critical behavior is observable in the high- $T_c$  materials because of the high temperatures and the very short pair coherence length. The glass transition is expected to be a second-order phase transition at  $T_g$ , characterized by a static scaling exponent  $\nu$  and a dynamic exponent  $z$ , which describe the divergent length and time scales of the vortex-vortex interaction:

$$\xi_{\text{VG}} \propto |T - T_g|^{-\nu} \quad \text{and} \quad \tau \propto \xi_{\text{VG}}^z. \quad (1)$$

As a consequence, the electric-field-current density isotherms obey a relation

$$E(J) \propto J \xi_{\text{VG}}^{d-2-z} E_{\pm} \left( \frac{J \xi_{\text{VG}}^{d-1} \phi_0}{ck_B T} \right), \quad (2)$$

where the  $E_{\pm}(x)$  are universal functions which characterize the system above and below the glass temperature. In the limit of small current density, where the system

behavior at large length scales is described, we expect  $E_+(x \rightarrow 0) \approx x$  so that the thermally activated flux-flow behavior of a liquid system is described and  $E_-(x \rightarrow 0) \approx e^{-x^{-\mu}}$ , which describes the glassy behavior of the system. At the glass temperature, in order that the diverging length scale cancels, the voltage-current isotherm has a power-law dependence,  $E(T_g) \propto J^{(z+1)/(d-1)}$ . The parameter  $d$ , assumed to be 3, is the dimensionality of the system.

The general behavior described above was first seen in thin-film  $\text{YBa}_2\text{Cu}_3\text{O}_{7-x}$  (YBaCuO) by Koch *et al.*<sup>1</sup> who obtained  $\nu = 1.7 \pm 0.2$  and  $z = 4.8$ , in general agreement with the theoretical prediction of Fisher, Fisher, and Huse.<sup>6</sup> These experiments have been repeated in other systems with reasonable agreement of the scaling exponents (see Table I), although the universality of the functions  $E_{\pm}(x)$  has been questioned. Gammel, Schneemeyer, and Bishop<sup>2</sup> point out a discrepancy between their data for single-crystal YBaCuO and that of Koch *et al.*<sup>1</sup> for thin-film YBaCuO. Most of the data published are confined to magnetic fields greater than about 0.1 T, and no authors suggest systematic dependence of the scaling exponents on the applied field in this field range. We present an investigation of scaling behavior at fields much lower than previously reported

TABLE I. Summary of  $\nu$  and  $z$  values for various YBaCuO systems.

System	Static exponent $\nu$	Dynamic exponent $z$	$2\nu_0$	Ref.
Film, 8- $\mu\text{m}$ bridge, 0.5-4 T	$1.7 \pm 0.2$	4.8		1
Single crystal, 1.5-6 T	$2 \pm 1$	$4.3 \pm 1.5$	1.33	2
Film, 2 T	1.9	4.8		4
Sintered polycrystal, 0.05-1.5 T	$1.1 \pm 0.2$	$4.6 \pm 0.2$		3
Single crystal, 0.1-9 T	$0.65 \pm 0.05$	$3 \pm 0.2$	1.26	12
Film, 10- $\mu\text{m}$ bridge, 4-6 T	$1.0 - 1.2$	4.8-6.0		13
Film, 5.6-0.54- $\mu\text{m}$ bridges, 1-3 T	$1.2 \pm 0.6 - 0.7 \pm 0.2$	$5.6 \pm 1.0 - 9.7 \pm 0.7$	$0.75 \pm 0.1 - 1.07 \pm 0.1$	7
Film, 50- $\mu\text{m}$ bridge				
0.015-5 T	$1.4 \pm 0.1$	$6.1 \pm 0.2$	1.5	this work
0-0.01 T	$1.1 \pm 0.1$	$8.3 \pm 0.3$		this work

and find that the data scale at all fields. At high fields our scaling exponents agree with those found by others. At low fields we find field-dependent exponents and a narrowing of the critical region. We point out one other case of anomalously high dynamic exponents<sup>8</sup> and compare our results.

## II. PROCEDURE

We measure dc voltage-current characteristics on a YBaCuO film<sup>9</sup> which is *c*-axis oriented, 110 nm thick, with a photolithographically etched 50- $\mu\text{m}$   $\times$  50- $\mu\text{m}$  bridge. The film is thermally sunk to a copper block that has platinum and carbon glass thermometers embedded in it. This sample housing is mounted in a variable temperature cryostat that routinely achieves a temperature stability of better than 10 mK. We evaporate gold pads onto the film and bond gold wires to them, forming current and voltage leads in a four-point configuration. Direct current is supplied by a Keithley 220 current source and the voltage is measured by a Keithley 182 nanovoltmeter. Thermal offsets are minimized by reversing the current direction, and the current is applied for only 1.8 s in each direction, which represents 10% of each measurement cycle. Each reading is an average of 30 voltage measurements. We increment the current logarithmically from a value where the voltage is below our resolution of 15 nV ( $\approx 3\mu\text{V cm}^{-1}$ ) to just below the critical current density. Each isotherm takes 15–20 min to generate. The isotherms are generally 100 mK apart except at ambient field, where they are more closely spaced.

The external magnetic field is applied to the *c* axis of the sample and is generated by a Cryomagnetics superconducting magnet. The magnet's power supply, the current source, and the nanovoltmeter are monitored and controlled remotely by LabView software on an Apple Macintosh system.

## III. DATA

Data were collected for fields ranging from 5 T to ambient field. At each field we map out isotherms on either side of  $T_g$ . We present our data in Figs. 1, 2, and 3 for 2.5 T, 10 mT, and ambient field, respectively. In each case, part (a) shows the  $\rho = E/J$  versus  $J$  isotherms, while part (b) of the figure is a plot of the scaled resistivity

$$\tilde{\rho} = \rho |1 - T/T_g|^{v(1-z)} \quad (3a)$$

against the scaled current density

$$\tilde{J} = \frac{J}{T} |1 - T/T_g|^{-2\nu} \quad (3b)$$

Evidently, by appropriate choice of scaling parameters  $T_g$ ,  $\nu$ , and  $z$ , each set of isotherms collapses nicely onto two  $\tilde{\rho}$  and  $\tilde{J}$  curves. The functions  $E_{\pm}$  represented by the curves look very similar to the forms published in the literature—in particular, the agreement with Ref. 5, Fig. 3, is excellent. At high fields, from 5 to 0.25 T, the scaled isotherms all have exactly the same form. At lower fields we judge the quality of the scaling to be the same, but the functions gradually change. This reflects the change in

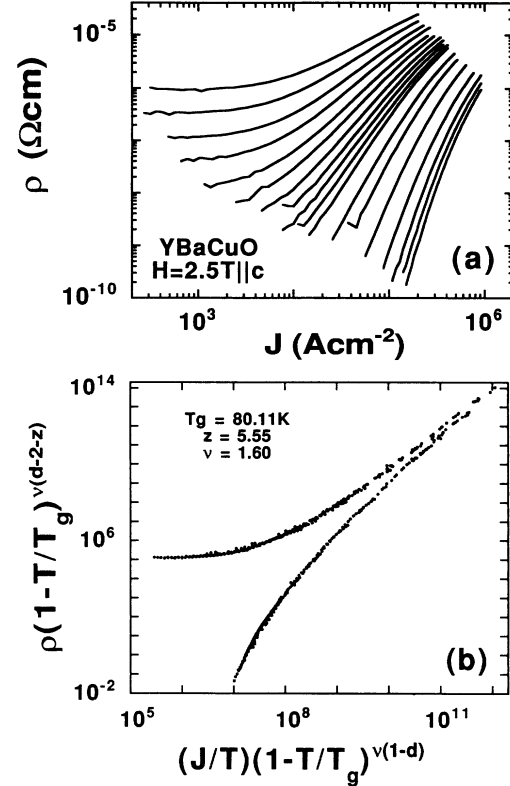


FIG. 1. (a)  $\rho$ - $J$  isotherms for a YBaCuO film with a 2.5-T field applied parallel to the *c* axis. The temperature range is 74.5–82.5 K. (b) Data in (a) scaled according to Eq. (3).

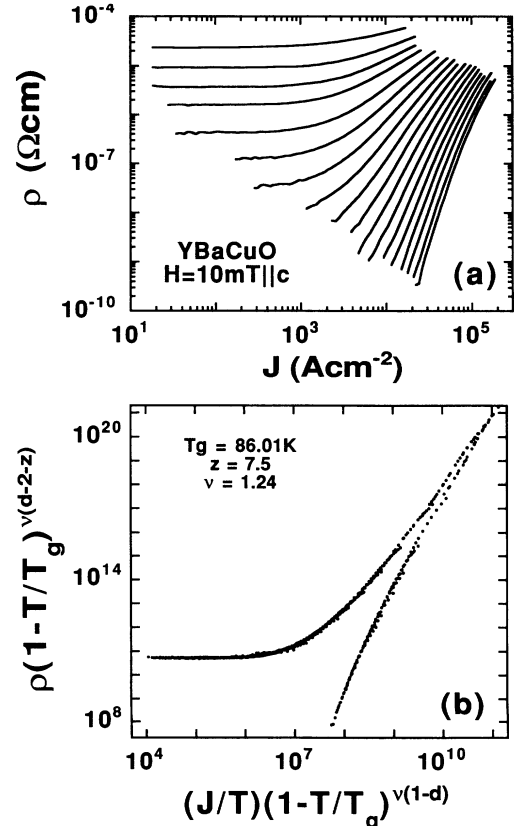


FIG. 2. (a)  $\rho$ - $J$  isotherms for a YBaCuO film with a 10-mT field applied parallel to the *c* axis. The temperature range is 85.4–86.8 K. (b) Data in (a) scaled according to Eq. (3).

the scaling exponents, especially an increase in  $z$ , discussed below.

The best scaling parameters were found in the same manner for each field. Vortex-glass theory predicts  $\rho$ - $J$  isotherms that become power-law-like at small distance scales (high current densities), but since all of the isotherms show downward curvature at sufficiently high current density (presumably where flux-flow effects dominate), some cutoff criterion is necessary. We generally choose a constant power criterion. Since the universal functions are not known, except in various limits, it is not possible to do a least-squares fit to the data, and so we choose the fitting parameters  $T_g$ ,  $\nu$ , and  $z$  in the following way. A range of acceptable  $T_g$  values is defined from those isotherms that show neither upward nor downward curvature at low currents, and one is chosen as the most likely critical isotherm. An initial value of the parameter  $z$  is obtained from the slope  $(z-1)/2$  of the critical  $\ln\rho$  versus  $\ln J$  isotherm. Then, for temperatures greater than  $T_g$ , the region of constant resistivity at low current density  $\rho_{\text{lin}} \equiv \lim_{J \rightarrow 0} (E/J)$  is examined. For each isotherm,  $\rho_{\text{lin}}$  is plotted against  $T - T_g$  on a log-log scale (see Fig. 4). The plot is linear in the critical regime, with a slope  $s = \nu(z-1)$ , which gives a value for  $\nu$  as  $\nu = s/(z-1)$ . (We do not include isotherms that fall outside of this linear regime in subsequent analysis.) The

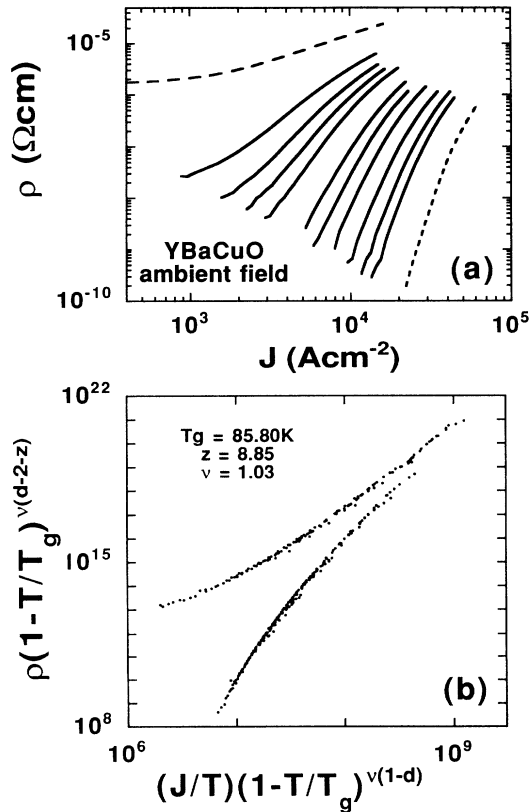


FIG. 3. (a)  $\rho$ - $J$  isotherms for a YBaCuO film at ambient field. The dashed lines indicate isotherms outside of the scaling region. The temperature range is 85.3–86.0 K for isotherms which are scaled. (b) Data in (a) scaled according to Eq. (3).

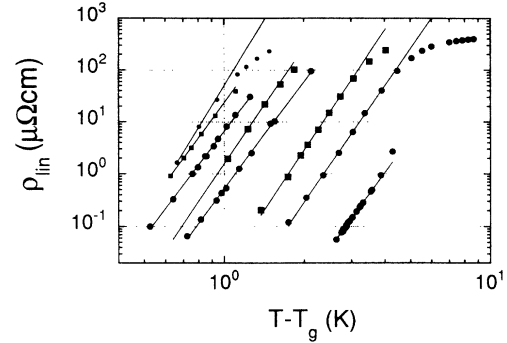


FIG. 4. Low-current resistivity  $\rho_{\text{lin}}$  as a function of  $(T - T_g)$ . A linear slope of this semilogarithmic plot indicates that the resistivity obeys the form predicted by vortex-glass theory. The data are for fields (from left to right) 0 T, 5 mT, 30 mT, 0.1 T, 0.25 T, 1 T, 2.5 T, and 5 T.

other candidates for the critical isotherm likewise yield trial values for  $T_g$ ,  $z$ ,  $s$ , and  $\nu$ . From here, the parameters are adjusted to obtain the best collapse of the data onto the two universal  $\tilde{\rho}$  versus  $\tilde{J}$  curves, always observing the constraints for  $T_g$  and the appropriate  $s$  for the field at hand. In general, we find that the initial estimation of  $T_g$  is very good, and the scaling procedure adjusts it by, at

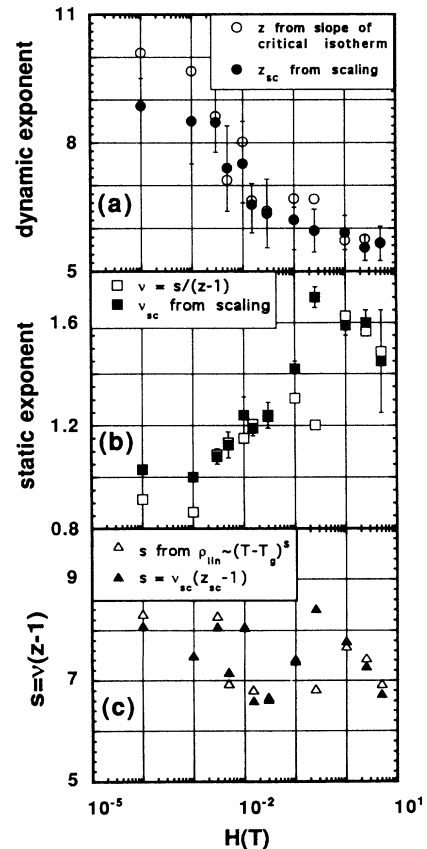


FIG. 5. Scaling parameters  $z$ ,  $\nu$ , and  $s$  at all the fields measured. The solid symbols denote values obtained from scaling the  $\rho$ - $J$  isotherms, while open symbols denote values obtained directly (see text).

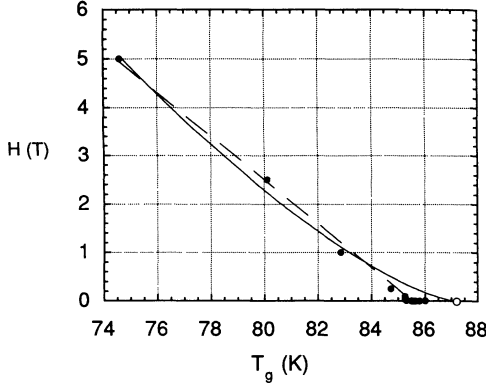


FIG. 6.  $H$ - $T$  phase diagram determined as described in the text. Solid circles denote  $T_g$  values. The ambient-field transition temperature (maximum of  $dR/dT$ ) is indicated by the open circle.

most, 70–100 mK.

At ambient field there is no temperature range in which the plot of  $\rho_{\text{lin}}$  versus  $T - T_g$  is linear. This does not indicate a lack of isotherms in the scaling region, but merely that the current density  $J_{\text{nl}}$  below which the resistivity becomes constant has fallen beneath the limit of detection (it falls off as  $|1 - T/T_g|^{2\nu}$ ). The lack of linearity sets an upper bound on the width of the critical region and a lower bound on the value of the parameter  $s$ .

It is difficult to quantify the quality of the collapse of the isotherms onto two single curves; the collapse is very sensitive to  $T_g$ , and the parameters are not all independent. We varied the different parameters until the fit deteriorated, which resulted in a consistent, albeit qualitative, error estimate. Examination of Fig. 5, which shows the field dependence of  $\nu$ ,  $z$ , and  $s$ , reveals that there is a systematic dependence of the exponents on the field, but that one could define a high-field region above about 10 mT in which the parameters are in agreement with other reported high-field values.

The field dependence of the scaling parameter  $T_g$  is depicted in Fig. 6. The mean field  $T_c = 87.2$  K (defined as the maximum in  $dR/dT$ ) in ambient field is also shown and does not coincide with the glass temperature as defined above. The dependence of  $H$  on  $T_g - T_g(0)$  or on  $T_g - T_c(0)$  is neither a single power law nor a linear function over the whole field range. In the high-field regime ( $H > 0.1$  T),  $H$  depends almost linearly on  $T_g$  as shown by the dashed line in Fig. 6. This region, with the inclusion of the mean-field transition temperature, can also be described by  $H \propto (T_g - T_c)^{2\nu_0}$ , with  $2\nu_0 = 1.5$ , which is the solid line in Fig. 6. The very-low-field ( $H < 0.1$  T) behavior is evidently quite different.

#### IV. DISCUSSION

The vortex-glass model predicts field-independent scaling exponents  $z \approx 4-7$  and  $\nu \approx 1-2$  for the universal scaling exponents.<sup>1,6</sup> The critical exponents found at the higher fields are consistent with this prediction, and although the product  $s = \nu(z - 1)$ , which describes the decrease of linear resistivity at low currents above  $T_g$ , is rel-

atively field independent, the scaling exponents  $\nu$  and  $z$  are field dependent, especially below about 10 mT. In particular, the parameter  $z$  becomes very large, which is equivalent to the statement that the slope of the critical isotherm becomes steeper with decreasing field. However, the good quality of the scaling collapse is maintained.

The critical region is less than 700 mK wide at ambient field. One expects the critical region to become smaller approximately as  $[H/H_{c2}(T)]^{2/3}$ ,<sup>7</sup> which for a field of  $10^{-4}$  T (ambient) gives a range of about several mK if we assume a critical region of about 8 K at high fields (see Fig. 4). This is well below our temperature resolution, and so we should not be able to scale any data at ambient field according to this criterion.

Zero-field  $E$ - $J$  curves have been reported in the literature with an attempt to extract scaling exponents from them.<sup>10</sup> There, the authors show data at 4 T and at zero field for a much thinner film (50 nm) than is used here or in most of the other work reported in the literature. They note deviations from the three-dimensional (3D) scaling forms at both fields, especially the lower, and attribute them to dimensional effects. For the zero-field data, they use the isotherms at high current density in the vicinity of the mean-field transition temperature to extract a value of  $z = 2.0$ , which is in agreement with the prediction of Ref. 6 for the transition to the Meissner state, but they do not explore the crossover from the high-field value of  $z = 4.6$ . In our case, dimensional effects should be absent because the film is thicker. However, our  $T_g$  is lower than the mean field  $T_c$  and our ambient field value of  $z$  is very large.

We have considered several possible reasons for the change in  $\nu$  and  $z$  with the field. The first is that the low-field data could be outside of the critical regime. This would imply that the linearity of the  $\rho_{\text{lin}}$  versus  $\ln(T - T_g)$  plot and the collapse of these isotherms in exactly the same fashion as the higher-field data is fortuitous, which is unlikely. The second reason is that a different mechanism might be responsible for the transition at the lower fields. The scaling relations [Eq. (1)] should apply to any second-order normal-to-superconducting phase transition, with the values of the critical exponents dependent upon the specific type of transition, or, more generally, to the universality class to which the transition belongs. If the mechanism that drives the transition is different at low fields, then the change in critical exponents could indicate a crossover between two different processes and not a violation of universality. The coherence length can be estimated as

$$\xi_{\text{VG}}^2 = \frac{k_B T}{\gamma J_{\text{nl}} \phi_0}, \quad (4)$$

where  $J_{\text{nl}}$  is the current density at which the resistivity above  $T_g$  begins to deviate from its constant, low-current value. If we set this equal to the average vortex spacing,

$$a_0 = \sqrt{\phi_0/B}, \quad (5)$$

and use Eq. (1), we find for each field a temperature at which  $\xi \approx a_0$ . At the highest fields, the scaled data are well within the temperature range for which  $\xi > a_0$ . At

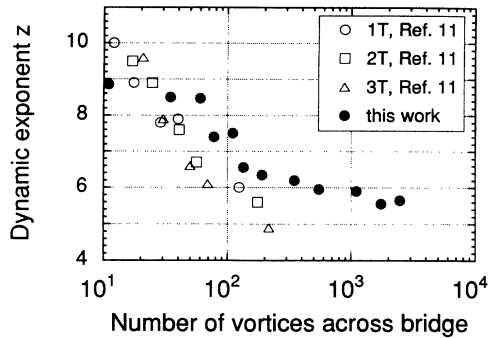


FIG. 7. Dynamic scaling exponent  $z$  as a function of number of vortices across the bridge. The solid circles are the values obtained from the scaling of the  $\rho$ - $J$  isotherms; the open symbols are from Refs. 8 and 11.

lower fields, the limit  $\xi \approx a_0$  is approached, and for ambient field, the uncertainty in the temperature range is large enough that we cannot exclude the possibility that some data may correspond to  $\xi < a_0$ . Thus, at higher fields, there are many vortices in a coherence length; at lower fields, for some of the scaled isotherms, there are few vortices in a coherence length, and at ambient field there may be less than 1. It seems reasonable that the physics should be different in the two limits. This possibility is suggested in Ref. 6 where it is noted that if  $a_0 \gg \xi_{VG}$ , the barrier for vortex recombination can be large, and that if the process is too slow to occur, then the universality class of the transition and the glass phase may change. Another relevant length scale is the penetration depth; at about 6 mT, the average vortex spacing becomes larger than the penetration depth.

A third possibility also relates to size effects. In a recent experiment,<sup>8</sup> Ando, Kubota, and Tanaka determined the vortex-liquid to vortex-glass phase transition parameters for very narrow microbridges. They observed a systematic increase in the dynamic exponent with decreasing bridge width. In their limited field range (1–3 T), they

also found a small field dependence.<sup>11</sup> At the lowest flux densities in our experiment, the intervortex spacing  $a_0$  approaches other length scales in the system, and so the number of vortices across our wider microbridge width is comparable to that in the Ando-Kubota-Tanaka experiment. If we plot the dynamic exponent as a function of the number of vortices across the bridge, as in Fig. 7, the agreement between the two experiments is striking. Ando, Kubota, and Tanaka suggested that the increased slope of the critical isotherm (increased  $z$ ) could be related to a softening of the vortex lattice. This softening, inferred from the systematic decrease in the value of  $T_g$  with film width at constant field, was explained by a reduced interaction energy density of vortices near the edge of the film. We could be observing a related effect since the elastic moduli of the vortex lattice decrease in the low-field region. It is also worth noting that, in contrast to our experiment, the large dynamic exponents observed in the Ando-Kubota-Tanaka experiment are not accompanied by a decrease in the critical region. There, the critical region remains several kelvin wide, even at the largest  $z$  values.

In summary, we have analyzed the  $E$ - $J$  characteristics of thin-film YBaCuO within the context of the vortex-glass theory and found that, at all fields down to ambient, there is a critical region within which the data can be scaled. The critical exponents are field dependent, especially at the lowest flux densities. The origin of this dependence and whether it represents a violation of the universality hypothesis is unsettled.

#### ACKNOWLEDGMENTS

We thank Dr. P. Berberich and Professor H. Kinder of the Technische Universität München for providing the YBaCuO film, and Dr. Y. Ando for discussion and for communicating unpublished results. We gratefully acknowledge assistance from D. W. Tom, J. Dille, and G. Karapetrov, and thank A. Stevenson for contributing to data analysis. J.T. acknowledges the financial support of the Alfred P. Sloan Foundation.

\*Present address: Freie Universität Berlin, D-14195 Berlin, Germany.

<sup>1</sup>R. H. Koch, V. Foglietti, W. J. Gallagher, G. Koren, A. Gupta, and M. P. A. Fisher, *Phys. Rev. Lett.* **63**, 1511 (1989).

<sup>2</sup>P. L. Gammel, L. F. Schneemeyer, and D. J. Bishop, *Phys. Rev. Lett.* **66**, 953 (1991).

<sup>3</sup>T. K. Worthington, E. Olsson, C. S. Nichols, T. M. Shaw, and D. R. Clarke, *Phys. Rev. B* **43**, 10 538 (1991).

<sup>4</sup>C. Dekker, P. J. M. Wöltgens, R. H. Koch, B. W. Hussey, and A. Gupta, *Phys. Rev. Lett.* **69**, 2712 (1992).

<sup>5</sup>P. J. M. Wöltgens, C. Dekker, J. Swüste, and H. J. de Wijn, *Phys. Rev. B* **48**, 16 826 (1993).

<sup>6</sup>D. S. Fisher, M. P. A. Fisher, and D. A. Huse, *Phys. Rev. B* **43**, 130 (1991).

<sup>7</sup>G. Blatter, M. V. Feigel'man, V. B. Geshkenbein, A. I. Larkin, and V. M. Vinokur (unpublished).

<sup>8</sup>Y. Ando, H. Kubota, and S. Tanaka, *Phys. Rev. Lett.* **69**, 2851 (1992).

<sup>9</sup>P. Berberich, J. Tate, W. Dietsche, and H. Kinder, *Appl. Phys. Lett.* **53**, 925 (1988).

<sup>10</sup>C. Dekker, R. H. Koch, B. Oh, and A. Gupta, *Physica C* **185-189**, 1799 (1991).

<sup>11</sup>Y. Ando (private communication).

<sup>12</sup>N.-C. Yeh, W. Jiang, D. S. Reed, U. Kriplani, F. Holtzberg, A. Gupta, and A. Kussmaul, in *Layered Superconductors: Fabrication, Properties and Applications*, edited by D. T. Shaw, T. R. Schneider, C. C. Tsuei, and Y. Shiohara, MRS Symposium Proceedings No. 275 (Materials Research Society, Pittsburgh, 1992), p. 169.

<sup>13</sup>R. M. Silver and A. L. de Lozanne, *IEEE Trans. Appl. Supercond.* **AS-3**, 1394 (1993).